

THE ONSET OF ROUGHNESS EFFECTS IN THE TRANSITIONALLY ROUGH REGIME

Karen A. Flack¹, Michael P. Schultz², William B. Rose²
Department of Mechanical Engineering¹
Department of Ocean Engineering and Naval Architecture²
United States Naval Academy
Annapolis, MD 21402 USA
flack@usna.edu, mschultz@usna.edu

ABSTRACT

Understanding the relationship between a surface's topography and its hydraulic resistance is an important, yet illusive, goal in fluids engineering. Particularly poorly understood are the flow conditions at which a given surface will begin to show the effects of roughness in the form of increased wall shear stress above that of the hydraulically smooth wall. This phenomenon is the focus of the present study. The results from a small scale fully-developed turbulent channel flow facility are presented for a hydraulically smooth wall and three rough surfaces (a sandpaper surface and two types of ship bottom paints). Experiments were conducted over a Reynolds number (Re_H) range of 3,200 – 64,000 based on the channel height and the bulk mean velocity. The onset of roughness effects occurs for the sandpaper surface at $k_{rms}^+ \sim 1$ or $k_s^+ \sim 5$, and this surface reaches fully rough conditions at $k_{rms}^+ \sim 12$ or $k_s^+ \sim 60$. Both these values of k_s^+ and the shape of the roughness function in the transitionally rough regime agree rather well with the results of Nikuradse (1933) for uniform sand. The frictional resistance of the two painted surfaces agrees within experimental uncertainty despite a factor of two difference in k_{rms} . The roughness functions for the painted surfaces do not exhibit either Nikuradse or Colebrook-type behavior. Further research is planned in which systematically varied roughness topographies will be tested. From this work, it is hoped that the roughness scales that most significantly contribute to the onset of roughness effects can be identified. Also planned are tests in a larger scale turbulent channel flow facility to map out the behavior of a range of roughness types from the hydraulically smooth to fully rough flow regime.

INTRODUCTION

Accurately predicting the increase in frictional drag due to surface roughness remains an important goal of fluids engineering research. Predictive models have been proposed for rough-wall flows in the fully rough regime, where pressure drag on the roughness elements dominates. However, the frictional drag behavior in the transitionally rough flow regime, where both viscous and pressure drag are both significant, is much more poorly understood. This is unfortunate since most engineering flows, including flows over ship hulls and turbine blades as well as fluid transport

typically operate in this regime. An important question in the transitional regime is how smooth is “hydraulically smooth”. Understanding the roughness scales that produce the onset of roughness effects is important for determining manufacturing tolerances and polishing levels necessary to produce test models that remain free of roughness effects. This is especially critical for flows operating at high unit Reynolds numbers. Currently, the onset of roughness effects and amount of additional drag due to roughness in the transitionally rough regime is only reliably known for a few surfaces that have been studied in detail. This leaves the frictional drag behavior of most surfaces in the transitionally rough regime unclear.

The amount of frictional drag due to surface roughness is dependent on many surface parameters including roughness height (k), shape, and density. A common measure of the momentum loss due to roughness is the roughness function (ΔU^+) which is the downward shift in the mean velocity profile when expressed in inner variables. A plot of ΔU^+ as a function of the roughness Reynolds number, $k^+ = kU_\tau/\nu$, for a wide range of surfaces (Flack and Schultz, 2010) indicates three distinct regimes (figure 1). When the roughness Reynolds number, k^+ , is small, the flow is hydraulically smooth (*i.e.* $\Delta U^+ = 0$). In this case the perturbations generated by the roughness elements are completely damped out by the fluid viscosity, creating no additional frictional drag. As k^+ increases, the flow begins to show the effects of the roughness and becomes transitionally rough. In the transitionally rough regime, viscosity is no longer able to damp out the turbulent eddies created by the roughness elements and form drag on the elements, as well as the viscous drag, contributes to the overall skin friction. As k^+ increases further, the roughness function reaches a linear asymptote. This asymptotic region at large values of k^+ is termed the fully rough regime. In this regime, the skin friction coefficient (c_f) is independent of Reynolds number, and form drag on the roughness elements is the dominant mechanism responsible for the momentum deficit in the boundary layer. The roughness functions for all surfaces will asymptote to a universal fully rough line if the equivalent sandgrain roughness height, k_s , is used as the characteristic roughness length scale, as shown in figure 2 (Flack and Schultz, 2010). The equivalent sandgrain roughness height is the roughness height that produces the same roughness function as the uniform sand roughness of Nikuradse (1933) in

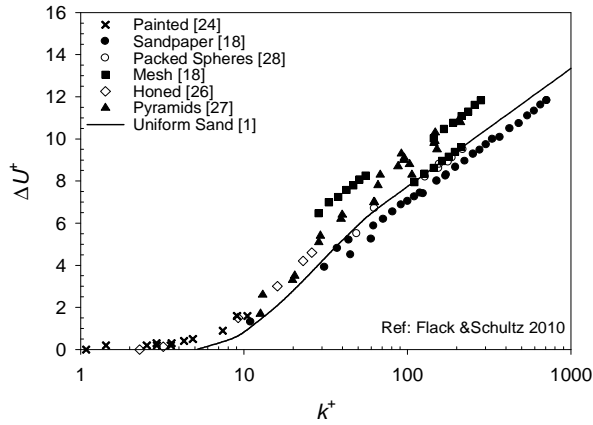


Figure 1. ΔU^+ vs. k^+

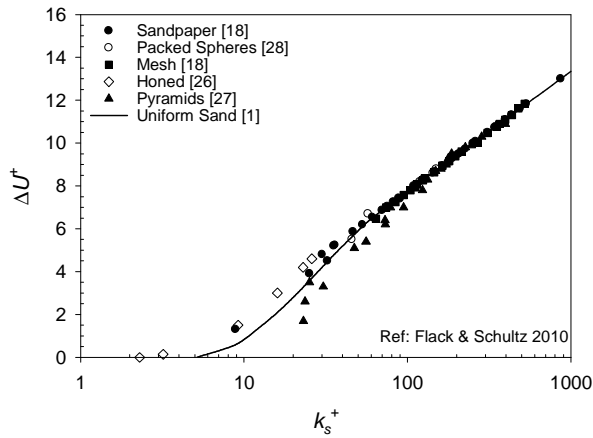


Figure 2. ΔU^+ vs. k_s^+

the fully rough regime. But, as indicated in figure 2, collapse in the fully rough regime does not ensure collapse in the transitionally rough regime.

A number of questions remain regarding the relationship between the roughness Reynolds number and the roughness function for a generic surface roughness. The value of k^+ (or k_s^+) when the surface roughness ceases to be hydraulically smooth has been shown to be a function of the roughness type. Secondly, the shape of the roughness function in the transitionally rough regime varies depending on roughness type and is not known for most surfaces. For example, some roughness types produce roughness functions with monotonically changing slope while others display inflectional behavior. Additionally, the value of k^+ that defines the start of the fully rough regime is unknown for most roughness types. The transitionally rough regime has previously been defined as $5 < k_s^+ < 70$, based on the uniform sandgrain results of Nikuradse (1933). However, a wide range of values has been reported in the literature for other roughness types. Ligrani and Moffat (1986) report that the transitionally rough regime spans $15 < k_s^+ < 50$ for a close-packed sphere bed. This range is reported as $3.5 < k_s^+ < 30$ for honed pipe roughness by Shockling, *et al.* (2006) and is given by Schultz and Flack

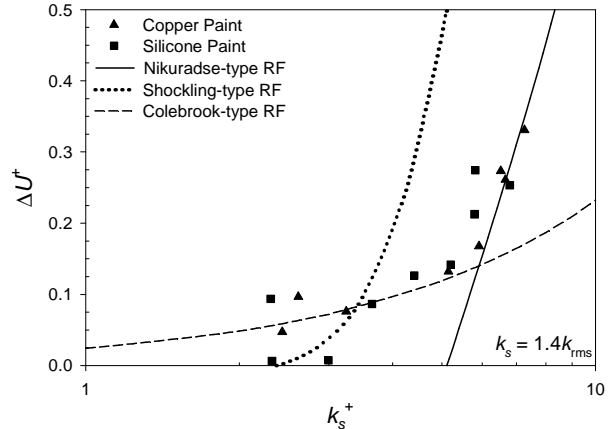


Figure 3. Roughness functions for ship bottom paints, boundary layer measurements

(2007) as $2.5 < k_s^+ < 25$ for a similar surface created by surface scratches. Langelandsvik, *et al.* (2008) indicate that the range of the transitionally rough regime is $1.4 < k_s^+ < 18$ for commercial steel pipe. Musker and Lewkowicz (1978) found that the onset of the fully rough regime ranged from $k_{rms}^+ = 17$ to 40 for ship-hull roughness.

The objective of the current research is to identify the roughness scales that contribute to the onset of roughness effects. Preliminary boundary layer measurements were taken to obtain the roughness functions in the transitionally rough regime for ship bottom paint (see Schultz and Flack, 2007 for experimental set-up). The results, shown in figure 3, indicate that ship bottom paint does not follow the previously proposed roughness functions (Nikuradse, 1933, Colebrook, 1939, Shockling, *et al.*, 2006). This underscores the need to test a range of roughness types and the difficulty in identifying the roughness scales that are applicable in the transitionally rough regime. The results also indicate that ship bottom paint deviates from hydraulically smooth at small values of k_s^+ . The scatter in the results for small k_s^+ also highlights the uncertainty in determining small changes in skin friction for mild roughness in a boundary layer flow. In rough-wall boundary layer investigations, it is difficult to determine the wall shear stress to better than $\pm 8\%$. A more accurate method of measuring the wall shear stress is necessary to determine the onset of roughness effects, especially for the case of mild roughness. Fully developed internal flows in pipes and channels allow the determination of the wall shear stress with greater accuracy using the streamwise pressure gradient.

EXPERIMENTAL METHODS

In order to address the challenge of detecting the small difference in wall shear stress, a fully-developed channel flow facility was constructed. A schematic of the test section is shown in figure 4. The channel has a height of 10 mm, a width of 80 mm, and a length of 1.6 m. The Reynolds number range is 3,200 – 64,000 (based on the channel height and the bulk mean velocity), providing a variation in the viscous length scale of 3.3 – 45 μm on a smooth wall. The facility has

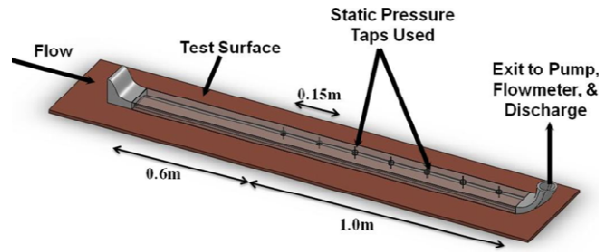


Figure 4. Schematic of Fully-Developed Channel Flow Facility

seven static pressure taps in the fully-developed region of the flow. The differential pressure transducers (GE Druck LPM9000) have a range of 0-20 inches water, with an accuracy of 0.1% of the reading. The flow meter (Yokagawa ADMAG AXF) has a range of 0-380 lpm, with an accuracy of 0.2% of reading. The pressure obtained at each location is the average of 30 seconds of collection at 50Hz. The mean wall shear stress is calculated from the measured pressure gradient in the channel, as shown in equation 1.

$$\tau_w = -\frac{H}{2} \frac{dP}{dx} \quad (1)$$

Measurements of the streamwise pressure gradient allows the wall stress to be determined within $\pm 1.5\%$.

Three sides of the channel are permanent and the fourth side is a removable test surface. The test surfaces investigated in this study are a smooth wall, the same ship bottom paints (copper and silicone) used in the boundary layer experiments and 220 grit sandpaper. While sandpaper has been extensively tested, it serves as a good surface for facility validation. The ship paints represent mild roughness with extensive engineering applications. Surface topographical maps are shown on figures 5-7. The surfaces were profiled with a Veeco Wyco NT9100 optical profilometer utilizing white light interferometry, with sub-micron vertical accuracy. The surface statistics of peak to trough roughness height (k_t), root-mean-square roughness height (k_{rms}), the skewness (Sk) and flatness (Ku) of the roughness probability density function (pdf) are listed on table 1. The surface statistics of k_{rms} and Sk were previously used by Flack and Schultz (2010) to predict the frictional drag on a rough surface in the fully rough regime.

RESULTS AND DISCUSSION

Skin friction results for a smooth test surface (figure 8) demonstrate good agreement with extant correlations for skin friction in a fully-developed, smooth-wall channel. Figure 8 shows the skin friction coefficient with a power law fit which compares well to the smooth wall power law correlation of Dean (1978), $c_f = 0.074Re^{-0.25}$. This high level of agreement is important to accurately determine the shear stress on the rough surfaces. For the rough walls, the wall shear stress obtained from pressure measurements represents an average of rough and smooth contributions since only one surface was covered

Table 1. Rough Surface Statistics

Specimen	k_t (μm)	k_{rms} (μm)	Sk	Ku
220-grit SP	212	28.1	0.272	4.09
Copper paint	140	20.5	-0.070	2.60
Silicone paint	60	10.0	0.127	2.84

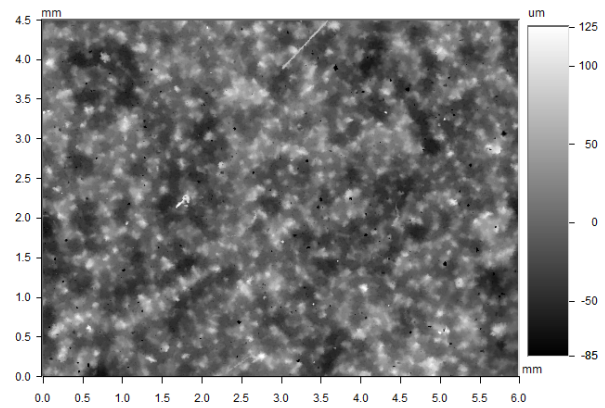


Figure 5. 220 grit sandpaper

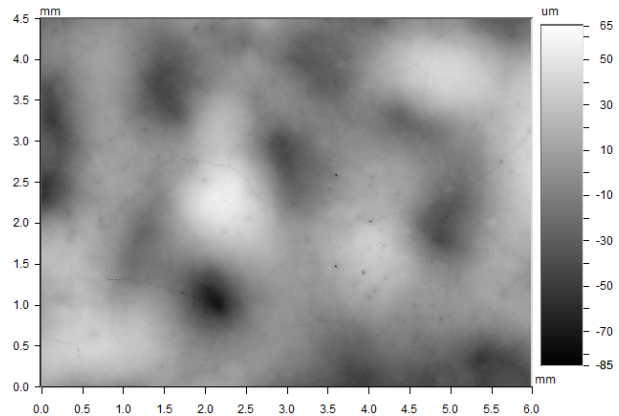


Figure 6. Copper paint

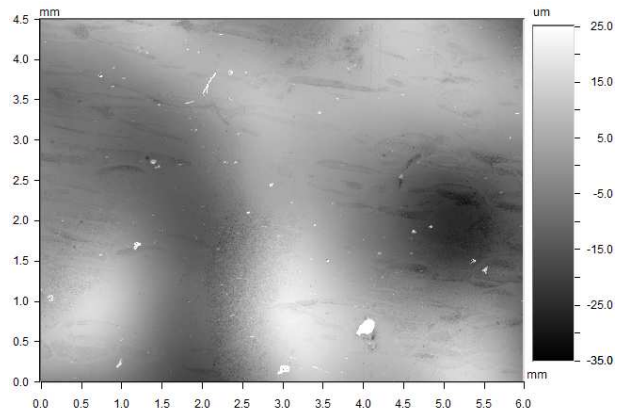


Figure 7. Silicone paint

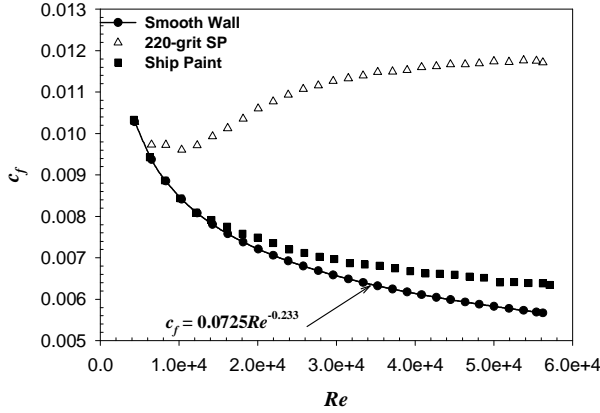


Figure 8. Skin-friction coefficients

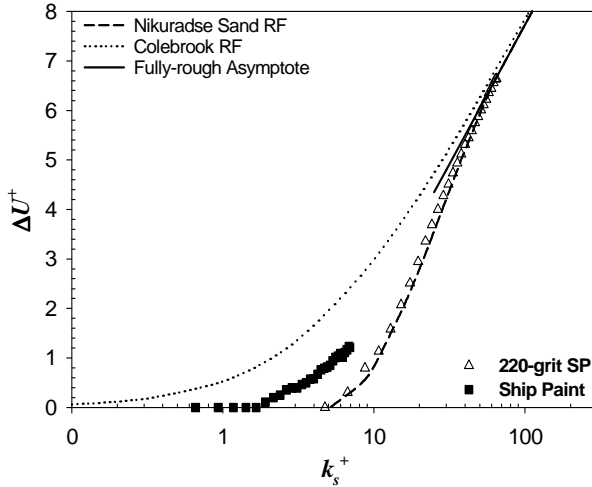


Figure 9. Roughness functions for rough surfaces

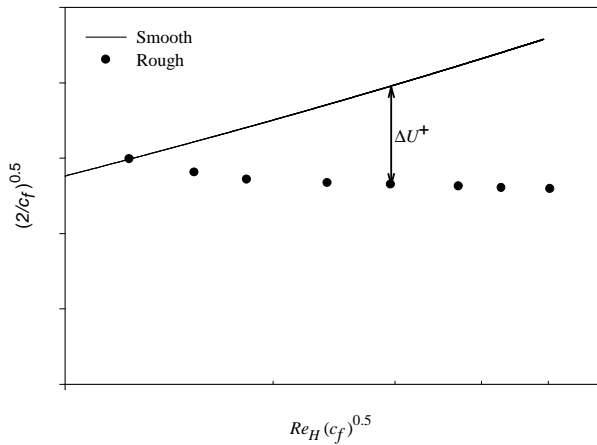


Figure 10. Determination of ΔU^+

with roughness. The smooth wall contribution, modeled using the power law correlation, is subtracted from the total, with the difference being the rough wall result. Skin friction results for the sandpaper and ship paints are also shown in figure 8. The copper and silicone ship paints yielded indistinguishable results within the measurement uncertainty of the facility. As expected from the roughness surface characteristics, the sandpaper skin friction deviates from the smooth wall at a significantly lower Reynolds number than the ship paints, resulting in large increases in wall friction. Much smaller differences are observed in skin friction for the ship paint as compared with the smooth wall. The ability to measure small differences and the overall smoothness of the results highlight the importance of determining the wall friction from a pressure drop in a channel as opposed to near wall boundary layer measurements. While this facility was constructed to determine the onset of roughness effects, results are presented over a wider Reynolds number range, indicating the fully rough regime for the sandpaper. The accuracy of the measurements beyond the onset of roughness effects will be determined when measurements are taken in a new, larger test section that can achieve higher Reynolds numbers and map the entire transitional regime. This facility is described in the future work section of this paper.

Roughness functions, ΔU^+ , for the three surfaces are shown on figure 9 for a range of roughness Reynolds numbers, $k_s^+ = \frac{k_s U_\tau}{\nu}$. Granville (1987) details the method of determining the roughness function for fully developed internal flows, shown schematically in figure 10. For the smooth wall, $\sqrt{\frac{2}{c_{f_s}}}$ is plotted vs. $Re_H \sqrt{c_f}$. A regression is performed on the smooth wall data yielding a power law equation. The roughness function is determined by taking the difference (Eqn. 2) at the same $Re_H \sqrt{c_f}$

$$\Delta U^+ = \sqrt{\frac{2}{c_{f_s}}} - \sqrt{\frac{2}{c_{f_R}}} \quad (2)$$

where $\sqrt{\frac{2}{c_{f_s}}}$ is based on the smooth wall equation and $\sqrt{\frac{2}{c_{f_R}}}$ is determined from the data for the rough wall. The friction velocity, $U_\tau = \sqrt{\frac{\tau_w}{\rho}}$, in the roughness Reynolds number is calculated from the measured pressure drop.

The results on figure 9 show that sandpaper roughness function departs from hydraulically smooth at $k_s^+ = 5$, consistent with the results of Nikuradse (1933). Additionally, the shape of the sandpaper roughness function is inflectional and closely follows the Nikuradse sand roughness function throughout the entire transitionally rough regime, as the data reaches the fully rough asymptote. The roughness functions for the copper and silicone ship paint indicate that the onset of roughness effects occurs at $k_s^+ = 2$, with numerous data points in the low roughness Reynolds number range. The boundary layer measurements of figure 3 showed this trend, but were not able to accurately capture the point of departure from hydraulically smooth.

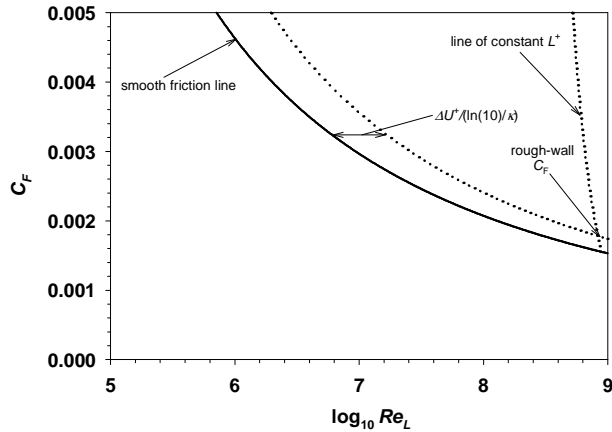


Figure 11. Scale-up procedure to determine the frictional drag coefficient

Schultz (2007) details the similarity methods used to determine the overall frictional resistance coefficient, C_F , for rough wall boundary layer flow over a flat plate of length L if the roughness function, ΔU^+ , is known. The methodology incorporates the analysis of Granville (1978, 1987) and relies on outer layer similarity in the mean flow for smooth and rough walls. A graphical representation of the scaling procedure is shown in figure 11. Here, the smooth wall overall frictional drag coefficient, C_F , is plotted as a function of $\log_{10}(Re_L)$ using the Karman-Schoenherr (1932) friction line, shown below.

$$\sqrt{\frac{2}{C_F}} = \frac{1}{\kappa} \ln(Re_L C_F) \quad (3)$$

The rough surface overall frictional resistance coefficient for a known roughness function is determined by displacing the smooth friction line by a distance $\Delta U^+ \kappa [\ln(10)]^{-1}$ in the positive $\log_{10}(Re_L)$ direction. For a given plate length, L , a line of constant $L^+ = LU_c v^{-1}$, which satisfies the following relationship is plotted.

$$Re_L = \frac{L^+}{\sqrt{\frac{C_F}{2} \left(1 - \frac{1}{\kappa} \sqrt{\frac{C_F}{2}} \right)}} \quad (4)$$

The intersection of this line and the rough surface line identifies C_F for the rough plate at a single value of Re_L for a given ΔU^+ . If this procedure is performed for a full scale destroyer (DDG-51, $L_{ship}=142$ m) the copper paint leads to an increase of 2.0% in the overall frictional drag coefficient, C_F at 15 kts and an increase of 5.6% at 30 kts compared to the hydraulically smooth condition.

CONCLUSIONS AND FUTURE WORK

A facility has been constructed that can accurately detect the point of departure from hydraulically smooth for a rough surface. The sandpaper, with a large k_{rms} and k_t demonstrated the influence of roughness at $k_s^+=5$. The milder ship paints deviated at lower roughness Reynolds numbers, $k_s^+=2$. The

small scale of this facility makes it ideal for testing a wide range of rough surfaces. Future tests will include additional mild roughness, including surface deposits and pitting. Experiments will also be performed on surfaces where the roughness density has been systematically changed. This will allow for further understanding of the roughness scales (i.e. roughness height, density parameter, moments of the roughness *pdf*) that result in a deviation from hydraulically smooth. It is hypothesized that the largest elements determine the k^+ at which the transitionally-rough regime begins. Additional experiments are needed to test this hypothesis.

While it is important to discern when a surface deviates from hydraulically smooth, the more important result for flow modeling is mapping the roughness function throughout the entire transitionally rough regime. Understanding the shape of the roughness function (monotonic, inflectional, etc.) within the transitional regime is important for predicting the effect of roughness over a wide Reynolds number range.

Measurements of the roughness function throughout the transitionally rough regime will be obtained using a larger scale channel facility. The channel has a height of 25 mm, a width of 200 mm, and a length of 4.0 m. The Reynolds number range that can be achieved in this facility is 10,000 – 280,000. The channel has ten static pressure taps in the fully-developed region of the flow, resulting in wall stress measurements within $\pm 1.5\%$. The wide range of roughness types investigated in the smaller facility will also be tested in the larger channel, mapping the roughness function from hydraulically smooth to fully rough. Both sets of experiments will give insight to the overall goal of predicting the frictional drag in the transitionally rough regime using appropriate scales that are based solely on surface statistics.

REFERENCES

- Dean R. B., 1978, "Reynolds number dependence of skin friction and other bulk flow variables in two-dimensional rectangular duct flow," *ASME Journal of Fluids Engineering*, Vol. 100, pp. 215-223.
- Colebrook, C. F., 1939, "Turbulent flow in pipes, with particular reference to the transitional region between smooth and rough wall laws," *Journal of the Institute of Civil Engineers*, Vol. 11, pp. 133-156.
- Flack, K. A. and Schultz, M. P., "Review of hydraulic roughness scales in the fully rough regime," *ASME Journal of Fluids Engineering*, **132**(4), Article #041203, 2010.
- Granville, P. S., 1978, "Similarity-law Characterization Methods for Arbitrary Hydrodynamic Roughness," *David W. Taylor Naval Ship Research and Development Center*, Report# 78-SPD-815-01.
- Granville, P. S., 1987, "Three indirect methods for the drag characterization of arbitrary rough surfaces on flat plates," *Journal of Ship Research*, Vol. 31, No. 1, pp. 70-77.
- Langelandsvik, L.I., Kunkel, G.J. & Smits, A.J., "Flow in a Commercial Steel Pipe," *Journal of Fluid Mechanics*, **595**: pp. 323-339, 2008.

Ligrani, P. M. & Moffat, R. J., Structure of Transitionally Rough and Fully Rough Turbulent Boundary Layers,” *Journal of Fluid Mechanics*, **162**, pp. 69-98, 1986.

Musker, A. J. & Lewkowicz, A. K., Universal Roughness Functions for Naturally-occurring Surfaces,” *Proceedings of the International Symposium on Ship Viscous Resistance-SSPA Goteborg, Sweden*, 1978.

Nikuradse, J., *NACA Technical Memorandum 1292*, 1933.

Schoennerr, K. E., 1932, “Resistances of Flat Surfaces Moving through a Fluid,” *Transactions SNAME*, **40**, pp. 279-313.

Schultz, M. P., 2007, “Effects of Coating Roughness and Biofouling on Ship Resistance and Powering,” *Biofouling*, **23**, pp. 331-341.

Schultz, M. P. & Flack, K. A., “The Rough-Wall Turbulent Boundary Layer from the Hydraulically Smooth to the Fully Rough Regime,” *Journal of Fluid Mechanics*, **580**, pp. 381-405, 2007.

Shockling, M. A., Allen, J. J. & Smits, A. J., “Roughness Effects in Turbulent Pipe Flow,” *Journal of Fluid Mechanics*, **564**, pp. 267-285, 2006.